Improvement of LiDAR Data Accuracy Using 12 Parameter Affine Transformation

Chien-Ting Wu[1]* Cheng-Yang Hsiao[2] Chun-Sung Chen[3]

ABSTRACT LiDAR data in a local coordinate system may need to be georeferenced and converted into a geographic or projected system. In coordinate transformation, the 7-parameter Helmet transformation method is usually used in measurements to eliminate the systematic errors made by a laser scanner. However, 7-parameter coordinate transformation assumes that there is only one scale error in all of the systematic errors. This study used 12 parameter affine transformation for coordinate transformation of airborne LiDAR data and terrestrial LiDAR data. The LiDAR data accuracy results upon 6-parameter similarity transformation, 7-parameter similarity transformation, and 12-parameter affine transformation were compared. The results showed that using 12-parameter affine transformation the airborne LiDAR and terrestrial LiDAR data have 2-3 times greater accuracy than do 7-parameter or 6-parameter transformations.

Key Words : LiDAR, coordinate transformation, 12-parameter, affine transformation.

Introduction

The data obtained from laser scanner operations are three-dimensional point data uniformly distributed over the surface of a measured object, generally called point cloud or LiDAR data. Each point data contains space coordinates, a reflection strength value, or RGB color. Since airborne or mobile laser scanners are integrated with Global Positioning System (GPS) and Inertial Navigation System (INS) information, any integration of coordination among the systems will result in errors, which will eventually be concealed in the obtained LiDAR data. The LiDAR data of a stationary terrestrial laser scanner (TLS) use coordinate information that takes an instrument laser source as its origin, and in the same way, systematic errors cannot be obtained from the information.

The LiDAR coordinate system, Geocentric (ECEF), local Cartesian coordinate, total station coordinate system, or other coordinate systems, are different coordinate systems; therefore, in order to study the difference between scanned LiDAR data point coordinates and coordinates measured by other instruments, as well as to achieve accurate analysis, a coordinate transformation must be conducted. Georeferencing is important for the integration of TLS data and its derived products, e.g. 3D models with other geospatial data (Reshetyuk 2009).

There are many coordinate transformation methods, for example, similarity transformation is a transformation mode that has identical scale factors in different directions, the affine transformation is a transformation mode where size, position and shape are changeable (Andrei 2006), while the 6 and 7 parameter Helmet transformations are most typical among 3D similarity transformations. This study used control points for coordinate transformation of strip adjusted airborne LiDAR data and TLS LiDAR data prior to coordinate transformation by the 12-parameter affine transformation mode. The accuracy results of LiDAR point cloud data obtained after 6-parameter, 7-parameter, and 12-parameter coordinate transformations were discussed.

〔1〕國立交通大學土木工程研究所
Department of Civil Engineering, National Chiao Tung University, Hsinchu, Taiwan, R.O.C.
〔2〕中興工程顧問社防災科技研究中心
Disaster Prevention Technology Research Center, Sinotech Engineering Consultants, Inc.
〔3〕健行科技大學 應用空間資訊系
Department of Geomatics, Chien Hsin University of Science and Technology, Taoyuan County, Taiwan, R.O.C.
* Corresponding Author. E-mail : Kenwu@uch.edu.tw

Literature Review and Theory

For airborne LiDAR, errors in point cloud data must be corrected in order to obtain high accuracy and practical LiDAR results. For example, to directly calibrate various instruments, Wehr and Lohr (1999) repeated tests to determine the setting angle of the laser scanner. The pitch angle, yaw, and lateral tilt angle were calibrated, respectively, in each iteration process. Burman (2000) designed strips in four different directions to scan a region, and calculate the strength and elevation values of the overlapped region in order to resolve the setting angle errors of the strips. Baltsavias (1999) provided details of the specification and parameter data of a commercial airborne LiDAR system, as shown in Table 1. When the carrier is a helicopter, the flight altitude is about 400 m, the plane accuracy is about 25 cm, and the elevation accuracy is about 15 cm; when the carrier is a light airplane, the flight altitude is about 1000 m, the plane accuracy is about 60 cm, and the elevation accuracy is about 20 cm.

The accuracy of adjusted airborne LiDAR data can be approximately 10cm~50cm(Chen et al. 2005; Chen 2005; Hodgson and Bresnahan 2004; Wu et al. 2008). Therefore, this study compared strip adjusted airborne LiDAR data with ground control points, and then used the ground control points to make 6-parameter, 7-parameter, and 12-parameter coordinate transformations of the airborne point cloud data. The transformed LiDAR data were compared with ground control points. The experiment of TLS used the reflection target center point observed by a total station to make 6-parameter, 7-parameter, and 12-parameter coordinate transformations and compared with control points observed by a total station.

Taking a TLS system as an example, the relation between the scanner coordinate system and the object space coordinate system is as shown in Figure 1, where S is the position of the scanner(origin of three-dimensional laser scanner coordinate system), Point P is the position of the point to be measured, Point O is the origin of the object space coordinate system, ρ is the distance between S and P, α is the vertical angle between Point S and Point P, and θ is the horizontal angle (Lichti et al. 2000).

The mathematical expression for transforming a scanner coordinate system to an object space coordinate system is expressed as Eq.1, where the given control-point coordinates of three or more object spaces are used for transformation (Lichti et al. 2000).

$$\vec{R}_p = M\vec{r}_p + \vec{R}_s \tag{1}$$

where

$\vec{r}_p = [x_p \quad y_p \quad z_p]^T$: Coordinate vector of Point P in scanner coordinate system.

$\vec{R}_p = [X_p \quad Y_p \quad Z_p]^T$: Coordinate vector of Point P in object space coordinate system.

$\vec{R}_s = [X_s \quad Y_s \quad Z_s]^T$: Coordinate vector of Origin S of scanner coordinate system in object space coordinate system.

There are many coordinate transformation methods, for example, the similarity transformation is a transformation mode with identical scale factors in different directions, and the affine transformation is a transformation mode where size, position, and shape are changeable (Andrei 2006). A unique affine matrix is obtained by multiplying the rotation matrix and translation matrix of various axis within a space, thus allowing the object to change with the affine matrix (Liao 2008).

Many cases of LiDAR data processing are applications of coordinate transformation. For example, Lichti et

Table 1 Commercial airborne LiDAR instrument accuracy (Baltsavias 1999)

	Range Accuracy (cm)	Elevation Accuracy (cm)	Horizontal Accuracy (m)
ALTM 1020	2	<15	1‰h
TopoSys II	1	<15	0.5‰h
FLI-MAP II	<5	<10	<0.1
AeroScan	2~4	20	0.3
ALTMS	<15	15-60	1-3

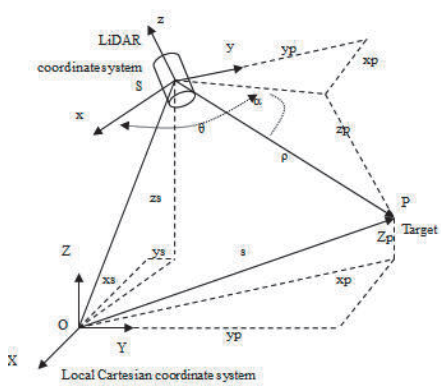

Fig.1 Relation between scanner coordinate system and object space coordinate system

al. (2000) tested a TLS three-dimensional monitoring network using 6-parameters transformation. Hsiao (2004) used 6-parameter transformation to transform TLS LiDAR data and detect landslide volume. Tsai (2007) used 6-parameters and 7-parameters transformation, with additional error parameters, to model possible systematic errors to determine error sources. Boeder et al. (2010) integrated two terrestrial laser scanning systems, the Zoller + FröhlichI MAGER 5006i and the Riegl VZ400, into a mobile hydrographical multi sensor system for hydrography.

12-parameter affine transformation (3D translation, 3D rotation, different scale factor along each axis and 3D skew) used to define relationship between two 3D image volumes. For instance, in medical image computing, the transformation model is part of different software programs that compute fully automatically the spatial transformation that maps points in one 3D image volume into their geometrically corresponding points in another, related 3D image volume (Maes et al. 1997).

Research Method

1. Coordinate transformation methods

Among the similarity transformations, the 6-parameter transformation converts three rotation angle parameters and three translation parameters (Eq. 2), whereas, the 7-parameter transformation involves one more scale factor (Eq. 3).

6-parameter transformation:

$$\begin{bmatrix} X_A \\ Y_A \\ Z_A \end{bmatrix} = \begin{bmatrix} x_0 \\ y_0 \\ z_0 \end{bmatrix} + R(\omega)R(\phi)R(\kappa)\begin{bmatrix} X_B \\ Y_B \\ Z_B \end{bmatrix} \quad (2)$$

7-parameter transformation:

$$\begin{bmatrix} X_A \\ Y_A \\ Z_A \end{bmatrix} = \begin{bmatrix} x_0 \\ y_0 \\ z_0 \end{bmatrix} + \lambda \times R(\omega)R(\phi)R(\kappa)\begin{bmatrix} X_B \\ Y_B \\ Z_B \end{bmatrix} \quad (3)$$

where

X_A, Y_A and Z_A are the given coordinates obtained by a total station (or the actual coordinates).

X_B, Y_B and Z_B are the observed coordinates obtained by a three-dimensional laser scanner.

x_0,y_0 and z_0 are the translation parameters of origin of the two coordinate systems.

λ is the scale parameter of the two coordinate systems.

Among the affine transformations, the 9-parameter transformation uses three translation parameters, three rotation parameters, and three scale parameters to build a three-dimensional model for geometric feature transformation (Niederöst 2001), as expressed in Eq. 4:

9-parameter transformation:

$$\begin{bmatrix} X_A \\ Y_A \\ Z_A \end{bmatrix} = \begin{bmatrix} x_0 \\ y_0 \\ z_0 \end{bmatrix} + S(\lambda_1)S(\lambda_2)S(\lambda_3) \times R(\omega)R(\phi)R(\kappa)\begin{bmatrix} X_B \\ Y_B \\ Z_B \end{bmatrix} \quad (4)$$

The 12-parameter transformation has three additional axis skew parameters, see Eq. 5:

$$\begin{bmatrix} X_A \\ Y_A \\ Z_A \end{bmatrix} = \begin{bmatrix} x_0 \\ y_0 \\ z_0 \end{bmatrix} + H(\theta_1)H(\theta_2)H(\theta_3) \times S(\lambda_1)S(\lambda_2)S(\lambda_3) \times R(\omega)R(\phi)R(\kappa)\begin{bmatrix} X_B \\ Y_B \\ Z_B \end{bmatrix} \quad (5)$$

where

X_A, Y_A and Z_A are the given coordinates obtained by a total station (or the actual coordinates).

X_B, Y_B and Z_B are the observed coordinates obtained by a three-dimensional laser scanner.

x_0, y_0 and z_0 are the translation parameters of origin of two coordinate systems.

λ_1, λ_2 and λ_3 are the scale parameters of the two coordinate systems.

θ_1, θ_2 and θ_3 are the skew parameters of the two coordinate systems.

The 7-parameter transformation can reduce the systematic errors, such as scale errors, of a three-dimensional laser scanner, as compared with a 6-parameter. The additional error parameters are helpful to some extent for correcting systematic errors in data (Tsai 2007).

Therefore, this study used 6-parameter and 7-parameter transformation to process scanned point cloud data, and applies the 12-parameter method for study. The accuracy relation between LiDAR data coordinates and actual coordinates is analyzed, the RMS in x, y, z axis and distance are used as accuracy evaluation indices. Table 2 shows the 6-parameter transformation results of the target center point coordinates of the TLS LiDAR reflection target 30 m away, which results contain the LiDAR coordinates, actual coordinates, transformed coordinates, and coordinate difference values.

2. Terrestrial LiDAR experiment design

The instrument for the TLS LiDAR experiments of this study was the Trimble MensiGS200 medium range three-dimensional laser scanner. The center point coordinates of the factory's reflection target can be directly determined by Trimble PointScape3.2 software in field operations.

The experimental site was an underground parking lot, where nine factory reflection targets were pasted on the metal plate and then pasted on the wall, arranged in a 3x3 matrix, as shown in Figure 2(a) and Figure 2(b). The total length of the parking lot was 90 m, which is within the scanning area of the three-dimensional laser scanner. There were three stages of scanning in this experiment, 30 m, 60 m, and 90 m, with each reflection target scanned 10 times, as shown in Figure 3.

TLS LiDAR reflection target accuracy was analyzed. The reflection target center point was observed by a total station and used as the actual coordinates. The TLS LiDAR reflection target center point coordinates were the observed coordinates. The coordinate difference values were compared after coordinate transformation.

Table 2 Results from the 6-parameter transformation of the target center point coordinates of a 30m reflection target (Unit : mm)

LiDAR X	LiDAR Y	LiDAR Z	Actual X	Actual Y	Actual Z	Transformed X	Transformed Y	Transformed Z	ΔX	ΔY	ΔZ
-4580.1	29502.9	1268.1	0.0	10567.0	410.8	-1.7	10567.3	410.9	1.7	-0.3	-0.1
-3849.3	29602.3	1265.5	752.6	10491.0	416.7	752.9	10490.8	416.8	-0.3	0.2	-0.1
:	:	:	:	:	:	:	:	:	:	:	:

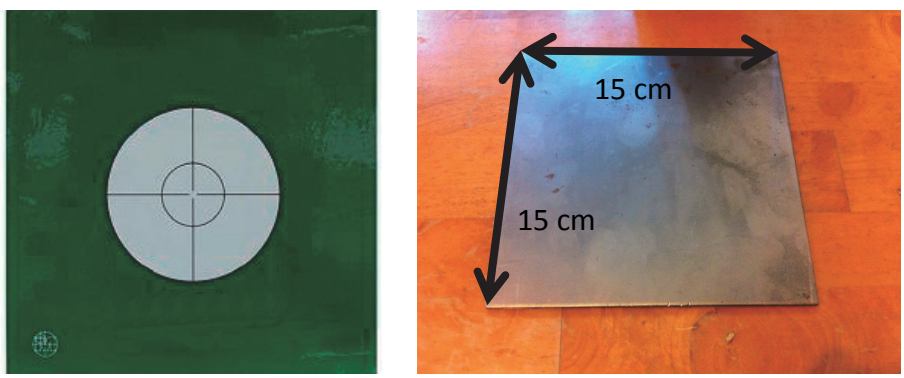

Fig.2(a) Reflection targets (left, 15cm x 15 cm) were pasted on the metal plate (right, 15cm x 15cm)

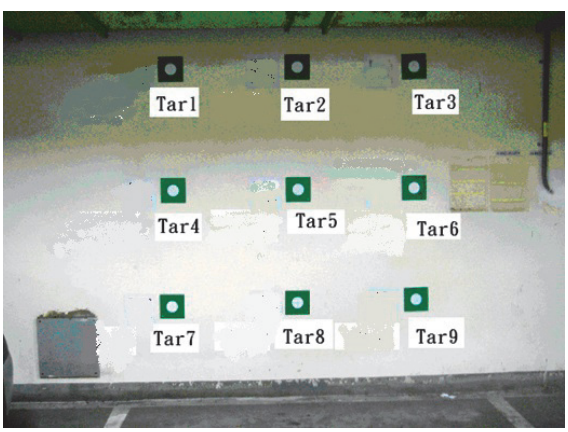

Fig.2(b) Layout of reflection targets

Fig.3 Three-dimensional laser scanner erected 30m away

The total station used in this experiment was a Leica TCR307 (see Figure 4), with the laser ranging in a non-reflecting prism mode, a distance accuracy of 3mm+2ppm in a non-reflecting prism mode, and angular accuracy of 7". The total station was erected about 10 m away from the reflection targets in the test site to observe the 9 reflection targets, record horizontal angle, vertical angle, and horizontal intervals, with the actual coordinates for the reflection targets obtained by trigonometric function calculation.

3. Airborne LiDAR experimental data

The airborne LiDAR point coordinate computations simultaneously obtained airborne GPS data and ground GPS station data, which were integrated with INS data to compute the optimal scanning trajectory, in real time three-dimensional coordinates and attitude parameters of each scanning strip. When point cloud data were generated, different systematic errors among the scanning strips rendered the overlapped zones mismatched, which phenomenon would result in discontinuity of the DEM and DSM of adjacent strips. Therefore, global strip adjustments must be conducted to render the data coincident (Hsiao et al. 2006).

Although systematic error correction was involved when airborne LiDAR point cloud data were generated, there would be systematic residual errors according to the overlap zone data accuracy analysis results, such as yaw, pitch, roll, and height errors of aircraft attitude. The accuracy of strip adjusted data must be re-evaluated to ensure the adjusted point cloud integrated data errors can be effectively reduced (Chen et al. 2005). In error evaluation, the overlapped zone data of several adjacent strips can be simultaneously selected, or the cross flight scanned overlapped data of normal strips can be used for error analysis. Finally, DSM and DEM were determined (Hsiao et al. 2006). The test zone was the airborne LiDAR data of Da-Guan, Taiwan, which is a mountainous area with large land modifications. The data were processed by strip adjustment and the noise point cloud is filtered, leaving only terrestrial point cloud data. The aerial photo of the test zone in Figure 5(a) and the results are shown in Figure 5(b).

Airborne LiDAR was collected at a flying height of 2106 meters above ground level (AGL) using an Optech ALTM (Airborne Laser Terrain Mapper) system. The red points are ground point data of airborne LiDAR data, the blue points are pass points, and the white points are ground control points. As observed, this operation covers five ground control points; however, as the airborne point cloud data are not regular grid point data, the point cloud data does not always fall on the center of control point, as shown in Figure 6.

Therefore, in order to check whether the airborne point cloud data are coincident with the ground control point, all point cloud data within the circle of ground control point, should be selected to take the average. The obtained coordinates are checked with the ground control

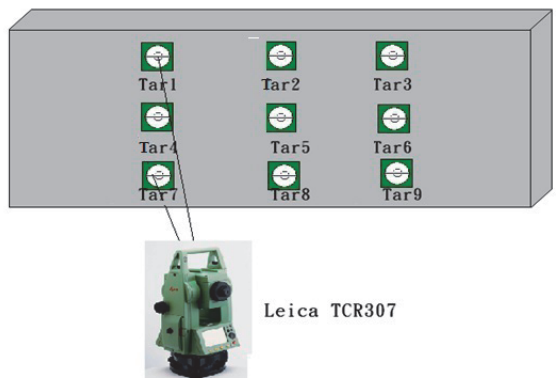

Fig.4 Schematic diagram of total station observing reflection targets

Fig.5(a) The aerial photo of the test zone

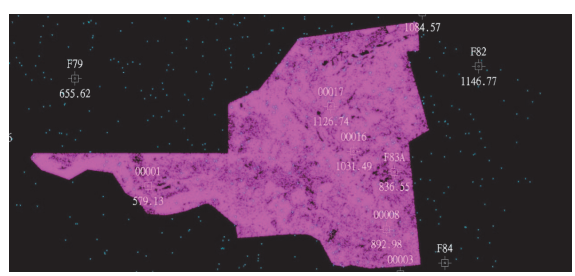

Fig.5(b) Airborne LiDAR test zone data

point. The five ground control points and airborne point cloud result data are preliminarily compared in Table 3.

Ground control points are standard data obtained from long-term GPS observations. According to the above table, the error in the airborne point cloud data is about 20cm~80cm, and the height (Z direction) difference is positive; however, there may be systematic errors. This study carried out 6-parameter, 7-parameter, and 12-parameter transformations based on the data, and converted the airborne point cloud coordinates into ground control point coordinates in order to compare the results after transformation.

Experimental Results

1. Terrestrial LiDAR experiment results

The terrestrial LiDAR experimental data are the unfiltered original data of reflection targets, with the nine reflection targets set at 30m, 60m, and 90m, for 6-parameter, 7-parameter, and 12-parameter transformations, respectively. The results after transformation are compared. Tables 4, 5, and 6 show the accuracy of the point cloud centers at 30m, 60m, and 90m after 6-parameter, 7-parameter, and 12-parameter coordinate transformations, respectively.

According to the above experimental data, there is no obvious difference in the RMS-s values of 6-parameter, 7-parameter, or 12-parameter at 30m. However, the 12-parameter affine transformation result is better than the 7-parameter similarity transformation at 60m and 90m, and the 7-parameter similarity transformation result is better than 6-parameter similarity transformation. According to the Table 5 and Table 6, the accuracy of 12-parameter is 2 times better than the accuracy of 7-parameter or 6-parameter transformations. The systematic errors of ground three-dimensional laser scanning can be reduced using 12-parameter affine transformation.

2. Airborne LiDAR experimental results

More than four control points are required for calculating 12-parameters, thus, the five navigation mark points are brought into 6-parameter, 7-parameter, and 12-parameter transformations. The results are shown in Tables 7~ 9.

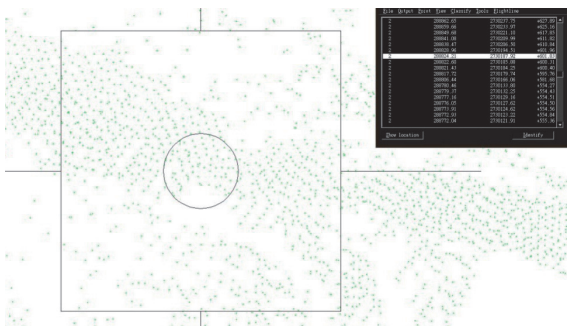

Fig.6 Schematic diagram of airborne LiDAR points and No.00001 ground control points (black frame and center circle)

Table 3 Comparison between airborne point cloud average coordinates and ground point coordinates (Unit: m)

Point Name	Pointcloud X	Pointcloud Y	Pointcloud Z	Ground point X	Ground point Y	Ground point h	ΔXi	ΔYi	ΔZi
00001	288824.21	2730187.92	601.83	288824.45	2730187.14	601.73	-0.24	0.78	0.1
00008	290438.28	2729908.95	915.79	290438.18	2729908.90	915.58	0.1	0.05	0.21
F83A	290491.84	2730278.58	859.40	290492.15	2730278.54	859.15	-0.31	0.04	0.25
00016	290215.98	2730409.97	1054.26	290216.26	2730410.07	1054.09	-0.28	-0.1	0.17
00017	290061.00	2730698.60	1149.48	290061.01	2730698.93	1149.34	-0.01	-0.33	0.14

Table 4 Accuracy of point cloud center at 30m after 6-parameter, 7-parameter, and 12-parameter coordinate transformations (Unit: mm)

	RMS-x	RMS-y	RMS-z	RMS-s
6-parameter	0.5665	0.4234	0.3694	0.7979
7-parameter	0.492	0.4214	0.3579	0.74
12-parameter	0.4261	0.7672	0.1648	0.8929

Table 5 Accuracy of point cloud center at 60m after 6-parameter, 7-parameter, and 12-parameter coordinate transformations (Unit: mm)

	RMS-x	RMS-y	RMS-z	RMS-s
6-parameter	10.4975	0.3336	4.8308	11.5605
7-parameter	7.3148	0.3938	6.0673	9.5118
12-parameter	4.5093	1.2340	1.5468	4.9244

According to the experimental airborne data, the result difference in the airborne LiDAR data is about 20cm~45cm after 6-parameter transformation, about 15cm~45cm after 7-parameter transformation, and about 5cm~18cm after 12-parameter transformation. As seen, the 7-parameter similarity transformation result is better than the 6-parameter similarity transformation, and the accuracy of 12-parameter transformation is 3 times better than the accuracy of 7-parameter transformation. Therefore, systematic errors of airborne data can be reduced through 12-parameter affine transformation using ground control points.

Conclusion

As seen in Tables 4 to 6, 7-parameter and 6-parameter coordinate transformations for terrestrial LiDAR data would result in different result accuracies. For example, the 7-parameter transformations and scale parameters are used in surveys to eliminate systematic errors of a laser scanner and increase accuracy. However, the 7-parameter coordinate transformation assumes that all systematic errors have only one scale error, and three rotation parameters and three translation parameters will not contain systematic errors, thus, all errors are corrected by one scale parameter. However, if the laser scanner or data have other systematic errors, they cannot be completely absorbed if there are only scale errors (Tsai 2007).

Regardless of airborne LiDAR or terrestrial LiDAR, a three-dimensional laser scanner uses its laser source as the origin of LiDAR coordinate system. The coordinate data of each point provided during data output. Therefore, users cannot know whether the coordinate system has other error factors, such as, whether the three axis are not orthogonal to each other at 90°, and whether the laser ranging or internal graduated circle has errors. The parameters of coordinate transformation will influence the result of external accuracy of data, the result of 6-parameter and two additional parameters is better than that of 7-parameter, and the result of 7-parameter and two additional parameters is better than that of 6-parameter and two additional parameters (Tsai 2007).

Table 6 Accuracy of point cloud center at 90m after 6-parameter, 7-parameter, and 12-parameter coordinate transformations (Unit: mm)

	RMS-x	RMS-y	RMS-z	RMS-s
6-parameter	17.0993	0.3736	6.0071	18.1277
7-parameter	11.1789	0.3714	10.7707	15.5278
12-parameter	3.5639	1.1410	5.7095	6.8265

Table 7 Transform airborne LiDAR data to navigation mark control points using 6-parameter (Unit: m)

Point Name	Pointcloud X	Pointcloud Y	Pointcloud Z	Ground point X	Ground point Y	Ground point h	Transformed X	Transformed Y	Transformed Z	ΔXi	ΔYi	ΔZi
00001	288824.21	2730187.92	601.83	288824.45	2730187.14	601.73	288824.3819	2730187.335	601.7378903	0.068	-0.195	-0.008
00008	290438.28	2729908.95	915.79	290438.18	2729908.9	915.58	290438.5565	2729909.005	915.7284675	-0.377	-0.105	-0.148
F83A	290491.84	2730278.58	859.4	290492.15	2730278.54	859.15	290491.9918	2730278.634	859.2132786	0.158	-0.094	-0.063
00016	290215.98	2730409.97	1054.26	290216.26	2730410.07	1054.09	290216.0958	2730409.998	1054.040169	0.164	0.072	0.050
00017	290061	2730698.6	1149.48	290061.01	2730698.93	1149.34	290061.0238	2730698.608	1149.170016	-0.014	0.322	0.170

Table 8 Transform airborne LiDAR data to navigation mark control points using 7-parameter (Unit: m)

Point Name	Pointcloud X	Pointcloud Y	Pointcloud Z	Ground point X	Ground point Y	Ground point h	Transformed X	Transformed Y	Transformed Z	ΔXi	ΔYi	ΔZi
00001	288824.21	2730187.92	601.83	288824.45	2730187.14	601.73	288824.3126	2730187.339	601.7148061	0.137	-0.199	0.015
00008	290438.28	2729908.95	915.79	290438.18	2729908.9	915.58	290438.5995	2729908.981	915.7297225	-0.420	-0.081	-0.150
F83A	290491.84	2730278.58	859.4	290492.15	2730278.54	859.15	290492.0407	2730278.636	859.2092077	0.109	-0.096	-0.059
00016	290215.98	2730409.97	1054.26	290216.26	2730410.07	1054.09	290216.1258	2730410.011	1054.049192	0.134	0.059	0.040
00017	290061	2730698.6	1149.48	290061.01	2730698.93	1149.34	290061.0443	2730698.643	1149.184587	-0.034	0.287	0.155

Table 9 Transform airborne LiDAR data to navigation mark control points using 12-parameter (Unit: m)

Point Name	Pointcloud X	Pointcloud Y	Pointcloud Z	Ground point X	Ground point Y	Ground point h	Transformed X	Transformed Y	Transformed Z	ΔXi	ΔYi	ΔZi
00001	288824.2	2730187.92	601.83	288824.5	2730187.14	601.73	288824.495	2730187.136	601.763427	-0.045	0.004	-0.033
00008	290438.3	2729908.95	915.79	290438.2	2729908.9	915.58	290438.319	2729908.887	915.611097	-0.139	0.013	-0.031
F83A	290491.8	2730278.58	859.4	290492.2	2730278.54	859.15	290492.063	2730278.486	859.195746	0.087	0.055	-0.046
00016	290216	2730409.97	1054.26	290216.3	2730410.07	1054.09	290216.095	2730410.117	1054.12457	0.165	-0.047	-0.035
00017	290061	2730698.6	1149.48	290061	2730698.93	1149.34	290061.146	2730698.884	1149.37585	-0.136	0.046	-0.036

However, 6-parameter or 7-parameter transformations are based on similarity transformation, which is a transformation mode with identical scale factors in various directions (Andrei 2006). If the three axis of the instrument are not orthogonal to each other, and the scales of the three axes are different, this study assumes that the instrument has systematic errors in orthogonality and systematic errors in scale of the three axes, and not just one scale error. The affine transformations, in which the size, position, and shape are changeable, can be used for increasing accuracy after transformation. The possible sources of various system errors include the instrument, the integrated system or the operating environment. Thus, future studies can establish parameters for different sources of system errors. Using 12-parameter and add additional parameters to estimate other sources of system errors could achieve better results.

LiDAR data can provide rapid high precision and high resolution 3D terrain information, in fields such as environmental surveys, monitoring, and disaster prevention and relief. For example, in the management of coastal zones, high-resolution elevation data play an important role. Changes of only a few dozen centimeters in elevation can produce significant changes in intertidal habitats, as well as the lives and properties of the people who live there. The monitoring of impounding dams requires 3D data with high precision and comprehensiveness. Regarding debris landslide areas, the accumulation areas and areas of debris flow activity, the topographic differences in these areas can be assessed and the changing trends explored using precise spatial database information. Hence, the 12 parameters of the proposed approach in this study could help improve the accuracy of Geodetics.

References

[1] 陳大科、蕭國鑫、石佳惠、王成機 (2005)，「空載光達資料航帶平差之精度探討」，第二十四屆測量學術及應用研討會論文集，123-132 頁。(Chen, D.K., Shio, K.S., Shih, J.H., and Wang, C.C. (2005). "Airborne LiDAR Systematic Error Analysis and Strip Adjustment." *24th conference on surveying and geomaticsTaiwan*. (in Chinese))

[2] 陳依萍 (2005)，「空載光達航帶平差方法分析比較」，國立成功大學測量及空間資訊研究所碩士論文。(Chen, Y.P. (2005). *Comparison and Analysis of Strip Adjustment Models for Airborne LIDAR*, Master thesis, The National Cheng Kung University, Tainan, Taiwan. (in Chinese))

[3] 廖珍鈺 (2008)，「三維動態網格壓縮與漸進式播放之研究」，中原大學資訊工程研究所碩士論文。(Liao, J.Y. (2008). *A Study on Progressive Compression of Animated 3D Mesh Models*, Master thesis, Chung Yuan Christian University, Taiwan. (in Chinese))

[4] 蔡漢龍 (2007)，「地面光達幾何校正系統設計與實施」，國立成功大學測量及空間資訊研究所碩士論文。(Tsai, H.L. (2007). *A Design and Its Implementation of Geometric Calibration System for Ground-based LiDARs*, Master thesis, The National Cheng Kung University, Taiwan. (in Chinese))

[5] 蕭國鑫、劉進金、游明芳、陳大科、徐偉城、王晉倫 (2006)，「結合空載 LiDAR 與航測高程資料應用於地形變化偵測」，航測及遙測學刊，第十一卷，第三期，283-295 頁。(Hsiao, K.H., Liu, J. K., Yu, M.F., Cheng, D.K., Hsu, W.C., and Wang, C.L. (2006). "Terrain Change Detection Combined Photogrammetric DEM and Airborne LiDAR Data." *Journal of Photogrammetry and Remote Sensing*, 11(3), 283-295. (in Chinese))

[6] Andrei, C.O. (2006). *3D affine coordinate transformations*, Master thesis, KTH Royal Institute of Technology, Stockholm, Sweden.

[7] Baltsavias, E.P. (1999). "Airborne laser scanning: basic relations and formulas." *ISPRS Journal of Photogrammetry & Remote Sensing*, 54, 199-214.

[8] Boeder, V., Kersten, T.P., Hesse, C., Thies, T., and Sauer, A. (2010). "Initial Experience with The Integration of a Terrestrial Laser Scanner into The Mobile Hydrographic Multi Sensor System on a Ship." *ISPRS Istanbul Workshop 2010 on Modeling of optical airborne and spaceborne Sensors*, Istanbul, Turkey.

[9] Burman, H. (2000). "Adjustment of Laser Scanner Data for Correction of Orientation Errors." *International Archives of Photogrammetry and Remote Sensing*, 33, 125-132.

[10] Hodgson, M.E., and Bresnahan, P. (2004). "Accuracy of Airborne Lidar-Derived Elevation: Empirical Assessment and Error Budget." *Photogr- ammetric Engineering & Remote Sensing*, 70(3), 331-339.

[11] Hsiao, K.H., Liu, J.K., Yu, M.F., and Tseng, Y.H. (2004). "Change Detection of Landside Terrians

Using Ground-Based LiDAR Data." *XXth ISPRS Congress*, Istanbul, Turkey.

[12] Lichti, D.D., Stewart, M.P., Tsakiri, M., and Snow, A.J. (2000). "Calibration and Testing of a Terrestrial Laser Scanner." *International Archives of Photogrammetry and Remote Sensing*, Amsterdam, The Netherlands, 485-492.

[13] Maes, F., Collignon, A., Vandermeulen, D., Marchal, G., and Suetens, P. (1997). "Multimodality image registration by maximization of mutual information." *IEEE transactions on Medical Imaging*, 16(2), 187-198.

[14] Niederöst, J. (2001). "3D reconstruction and accuracy analysis of historical relief models from the 18th century." *3rd International Image Sensing Seminar on New Development in Digital Photogrammetry,* Gifu, Japan.

[15] Reshetyuk, Y. (2009). *Self-calibration and direct georeferencing in terrestrial laser scanning*. Ph.D. Dissertation, KTH Royal Institute of Technology, Stockholm, Sweden.

[16] Wehr, A., and Lohr, U. (1999). "Airborne laser scanning - an introduction and overview." *ISPRS Journal of Photogrammetry & Remote Sensing*, 54, 68-82.

[17] Wu, J., Ma, H., and Li, Q. (2008) "Least Squares Matching with Airborne LiDAR Data for Strip Adjustment." *The International Archives of the Photogrammetry*, Remote Sensing and Spatial Information Sciences, Vol. XXXVII. Part B3b. Beijing, 167-171.

2012 年 08 月 13 日　收稿
2012 年 09 月 11 日　修正
2013 年 07 月 22 日　接受
(本文開放討論至 2013 年 6 月 30 日)